Title

Assessment of mechanical properties of articular cartilage with quantitative three-dimensional ultrashort echo time (UTE) cones magnetic resonance imaging

Authors

Namiranian, Behnam
Jerban, Saeed
Ma, Yajun
et al.

Publication Date

2020-12-01

DOI

10.1016/j.jbiomech.2020.110085

Peer reviewed

HHS Public Access

Author manuscript

J Biomech. Author manuscript; available in PMC 2021 December 02.

Published in final edited form as:

J Biomech. 2020 December 02; 113: 110085. doi:10.1016/j.jbiomech.2020.110085.

Assessment of mechanical properties of articular cartilage with quantitative three-dimensional ultrashort echo time (UTE) Cones magnetic resonance imaging

Behnam Namiranian[1,†], **Saeed Jerban**[1,†,*], **Yajun Ma**[1], **Erik W. Dorthe**[2], **Amir Masoud-Afsahi**[1], **Jonathan Wong**[3], **Zhao Wei**[1], **Yanjun Chen**[1], **Darryl D'Lima**[2], **Eric Y. Chang**[3,1], **Jiang Du**[1,*]

[1]Department of Radiology, University of California San Diego, San Diego, CA 92093, USA

[2]Shiley Center for Orthopedic Research and Education at Scripps Clinic, La Jolla, CA 92037, USA

[3]Research Service, VA San Diego Healthcare System, San Diego, CA 92161, USA

Abstract

Conventional magnetic resonance imaging (MRI) is not capable of detecting signal from the deep cartilage due to its short transverse relaxation time (T2). Moreover, several quantitative MRI techniques are significantly influenced by the magic angle effect. The combinations of ultrashort echo time (UTE) MRI with magnetization transfer (UTE-MT) and Adiabatic $T_{1\rho}$ (UTE-Adiab$T_{1\rho}$) imaging allow magic angle-insensitive assessments of all regions of articular cartilage. The purpose of this study was to investigate the correlations between quantitative three-dimensional UTE MRI biomarkers and mechanical properties of human tibiofemoral cartilage specimens. In total, 40 human tibiofemoral cartilage specimens were harvested from three male and four female donors (64±18 years old). Cartilage samples were scanned using a series of quantitative 3D UTE Cones T_2* (UTE-T_2*), T_1 (UTE-T_1), UTE-Adiab$T_{1\rho}$, and UTE-MT sequences in a standard knee coil on a clinical 3T scanner. UTE-MT data were acquired with a series of MT powers and frequency offsets to calculate magnetization transfer ratio (MTR), as well as macromolecular fraction (MMF) and macromolecular T_2 (T_2mm) through modeling. Cartilage stiffness and Hayes elastic modulus were measured using indentation tests. Correlations of 3D UTE Cones MRI measurements in the superficial layer, deep layer, and global regions of interest (ROIs) with mechanical properties were investigated. Cartilage mechanical properties demonstrated highest correlations with UTE measures of the superficial layer of cartilage. Adiab$T_{1\rho}$, MTR, and MMF in

[*]**Corresponding author: • Jiang Du**, Department of Radiology, University of California San Diego, 9500 Gilman Drive, San Diego, CA 92093, USA, jiangdu@ucsd.edu, Phone: +1 858 246 2248, Fax: +1 888 960 5922, **• Saeed Jerban**, Department of Radiology, University of California, 9500 Gilman Dr., San Diego, CA 92093, USA, sjerban@ucsd.edu, Phone : +1 858 246 3158, Fax : +1 888 960 5922.

[†]Behnam Namiranian and Saeed Jerban contributed equally to this work.

6. Conflict of interest statement

The authors have no conflicts of interest to declare.

superficial layer ROIs showed significant correlations with Hayes elastic modulus ($p<0.05$, $R=-0.54$, 0.49, and 0.66, respectively). These UTE measures in global ROIs showed significant, though slightly lower, correlations with Hayes elastic modulus ($p<0.05$, $R=-0.37$, 0.52, and 0.60, respectively). Correlations between other UTE MRI measurements (T_2*, T_1, and T_2mm) and mechanical properties were non-significant. The 3D UTE-Adiab$T_{1\rho}$ and UTE-MT sequences were highlighted as promising surrogates for non-invasive assessment of cartilage mechanical properties. MMF from UTE-MT modeling showed the highest correlations with cartilage mechanics.

Keywords

articular cartilage; ultrashort echo time; magnetization transfer; Adiab$T_{1\rho}$; mechanical properties; indentation test

1. Introduction

Articular cartilage is one of the most important components of the human knee joint, distributing compressive loads and enabling low-friction motion (Heinegård and Saxne, 2011). Two major macromolecular components of cartilage that can determine the joint's mechanical properties are collagen and proteoglycan (PG) (Sophia Fox et al., 2009). The collagen network of the cartilage primarily controls the dynamic response, while PG is responsible for the static mechanical properties of cartilage (Laasanen et al., 2003). Changes in collagen and PG in cartilage are expected to affect its biomechanical status (Li et al., 2010).

Osteoarthritis (OA) is the most common degenerative joint disease, with major impacts on quality of life, public health, and healthcare costs (Helmick et al., 2008; Yelin and Callahan, 1995). Important biochemical and microscopic signs of OA in its early stages include loss of PG, changes in collagen microstructure, and increases in water content (Kleeman et al., 2005). These changes increase the permeability and decrease the mechanical stiffness of cartilage (Kleeman et al., 2005). Softened cartilage is prone to both fissures and further fibrillation as it fails to resist impact forces during normal loading (Palmoski and Brandt, 1981). It is crucially important to develop accurate methods for non-invasive assessment of cartilage in early stages OA which can potentially facilitate timely interventions (Svärd et al., 2018).

Magnetic resonance imaging (MRI) is a non-invasive technique for OA diagnosis. MRI can provide accurate morphological assessment with high spatial resolution and soft tissue contrast (Bredella et al., 1999; Guermazi et al., 2011; Recht et al., 2005). Cartilage possesses a high percentage of organized collagenous matrix, particularly at the deep layer region, which results, in turn, in very short T_2 (Chang et al., 2015). Conventional MRI is not able to acquire short T_2 signals; therefore, accurate cartilage quantifications, such as the measurement of longitudinal (T_1) or transverse (T_2 or T_2*) relaxation times are challenging, especially for deep cartilage (Du et al., 2009). Furthermore, conventional quantitative MRI biomarkers, such as T_2 and $T_{1\rho}$, are sensitive to tissue orientation in the scanner due to the magic angle effect. Both T_2 and $T_{1\rho}$ values may increase drastically when the collagen fibers

are oriented from 0° to 55° relative to the B0 field. Specifically, For human cartilage specimens, different ranges of magic angle-related T2 variation have been reported, including 233% (Shao et al., 2017), 47% (Wang and Xia, 2013), and 21% on average (Li et al., 2011). Likewise for $T_{1\rho}$, different ranges of magic angle-related variation have been reported including 76% (Wu et al., 2020b), 92% (Shao et al., 2017), 32% (Wang and Xia, 2013), and 11% (Li et al., 2011). This magic angle-induced increase can far exceed changes caused by degeneration, which are typically in the range of 10–30% (Mosher et al., 2011), thereby complicating diagnosis and treatment monitoring based on MR quantitative techniques. As a result, conventional MRI techniques have limited success in assessing mechanical properties of articular cartilage, partly because of their inability to detect signal from the deep cartilage and partly because of the strong magic angle effect.

All regions of cartilage can be imaged by ultrashort echo time (UTE) MRI techniques (Chang et al., 2015; Juras et al., 2012). In UTE MRI, signal can be detected at an echo time as short as 8 μs (Chang et al., 2015). As a result, MR signal from otherwise “invisible” tissues with very short T_2 values can now be acquired and imaged with high signal intensity. Nevertheless, regular UTE biomarkers, such as UTE $T_{1\rho}$ and T_2*, are also prone to errors caused by the magic angle effect, resulting in drastic changes in MR quantifications due simply to alterations in angular orientation (Chang et al., 2016; Shao et al., 2017).

A novel $T_{1\rho}$ sequence has been recently developed using an adiabatic inversion recovery spin-lock pulse cluster followed by 3D-UTE-Cones data acquisition (3D-UTE-Adiab$T_{1\rho}$) (Ma et al., 2018a). Adiabatic pulses provide a robust spin-lock with much reduced sensitivity to B1 inhomogeneity. Recent studies showed that the adiabatic spin-lock can measure $T_{1\rho}$ with low-sensitivity to the magic angle effect (Ma et al., 2018a; Wu et al., 2020b). However, the relationship between UTE-Adiab$T_{1\rho}$ relaxation time and cartilage mechanical properties has not yet been investigated.

UTE MRI combined with magnetization transfer (UTE-MT) has also been recently proposed to quantify the macromolecular content relative to water content in the tissue (Ma et al., 2016; Y. Ma et al., 2017b). UTE-MT modeling relies on the phenomenon of magnetization transfer to quantify protons, including directly detected water protons and indirectly detected macromolecular protons, which possess T_2* values too short for direct imaging with current MRI techniques. UTE-MT modeling provides multiple parameters, including macromolecular fraction (MMF), macromolecular relaxation time (T_2mm), and exchange rates. Recent studies also demonstrate that UTE-MT modeling is insensitive to the magic angle effect (Ma et al., 2016; Zhu et al., 2018), supporting its potential for effective detection of cartilage degeneration. However, the relationship between two-pool MT modeling parameters and cartilage mechanical properties has not yet been investigated.

The present study aimed to investigate the relationship between a series of quantitative 3D-UTE-Cones MRI techniques (UTE-Adiab$T_{1\rho}$, UTE-T_2*, UTE-T_1, UTE-MT) and mechanical properties of human tibiofemoral cartilage. UTE MRI-based prediction of cartilage mechanical properties, as measured with an indentation test, could introduce these techniques as a potential new non-invasive tool for quantifying cartilage biomechanics and for the detection of cartilage degeneration.

2. Materials and Methods

2.1. Sample preparation

Tibial plateau and femoral condyle were dissected from seven fresh-frozen knee joints obtained from three male donors (88, 87, 48 years old) and four female donors (42, 68, 47, 57 years old). Frozen knee joints were provided by a non-profit whole-body donation company (United Tissue Network, Phoenix, AZ). Tibial plateau and femoral condyle were cut into rectangular cubes containing an approximately 14×14 mm^2 cross-section of tibiofemoral cartilage and the attached subchondral bone. The cut specimens were spaced at least 5 mm from the tibial plateau and femoral condyle edges. The total number of specimens was 40 (3–9 samples per donor). Next, the subchondral side of each specimen was resected using a low-speed diamond saw (Isomet 1000, Buehler, IL, USA) in order to obtain specimens with a thin subchondral bone layer (<5mm thick). The final dimension of specimens was approximately 14×14×7 mm^3. All cartilage specimens were macroscopically normal.

2.2. UTE MR Imaging

The 3D-UTE-Cones MRI scans were performed on a 3T MRI scanner (MR750, GE Healthcare Technologies, WI, USA) using an eight-channel knee coil (one RF transmission channel and eight signal reception channels). The cartilage specimens were soaked in phosphate-buffered saline (PBS) for 12 hours to ensure adequate rehydration after potential drying throughout the sample preparation. All specimens were placed in a plastic container filled with perfluoropolyether (Fomblin, Ausimont, NJ, USA) to minimize dehydration and susceptibility artifacts during MRI scans. The scans were performed at room temperature. The container was positioned carefully inside the knee coil to ensure that a major portion of the radial cartilage fibers were oriented parallel to B0 (cartilage surface was placed perpendicular to B0, similar to sagittal whole knee scan). All MRI images were acquired in the coronal plane.

Four sets of 3D-UTE-Cones MRI sequences were performed on the specimens: A) To measure T_2* values, a 3D-UTE-Cones T_2* sequence was performed with the following parameters: TR=100ms; flip angle (FA)=10°; fat saturation; multi-echoes with TEs of 0.032, 6.0, 11.6, 17.4, 23.2, and 29.0ms; and a scan time of approximately 6 minutes. B) To measure Adiab$T_{1\rho}$ values, seven 3D-UTE-Cones Adiab$T_{1\rho}$ sequences were performed with the following parameters: TR=500 ms; FA=10°, number of spokes=25; spin-locking time (TSL)=0, 12, 24, 36, 48, 72, and 96ms; number of adiabatic full passage (AFP) pulses=0, 2, 4, 6, 8, 12, and 16. The total approximate scan time for UTE-Adiab$T_{1\rho}$ was 30 minutes. C) To measure T_1, an actual flip angle imaging with variable TR (AFI-VTR)-based 3D-UTE-Cones sequence (AFI: TE=0.032 ms; TRs=20 and 100 ms; FA=45°; VFA: TE=0.032 ms; TRs=20 ms; FA=5, 10, 20, 30°; rectangular RF pulse with a duration of 150 μs) was performed with a total scan time of 30 minutes (Ma et al., 2018b). D) Additionally, a 3D-UTE-Cones MT sequence (Fermi saturation pulse power=500°, 1000°, and 1500°; frequency offset=2, 5, 10, 20, and 50 kHz; FA=7°; 9 spokes per MT preparation; rectangular RF excitation pulse of 100 μs) was performed for MT ratio (MTR) measurements and two-pool MT modelling with a total scan time of 25 minutes (Ma et al., 2016; Y. Ma et al., 2017b).

The total approximate scan time for this experiment was 90 minutes. Other imaging parameters included: field of view (FOV)=110mm×110mm, acquisition matrix=300×300, slice thickness=0.8 mm, number of slices=36, receiver bandwidth=±62.5 kHz. The MRI parameters for the performed sequences are summarized in Table 1.

2.3. MRI data analysis

UTE MRI quantifications were calculated in three representative slices at the middle of each specimen within three regions of interest (ROIs) which are schematically illustrated in Figure 2a: first, covering superficial layer (~1/3 of the cartilage thickness), R1 (superficial layer ROI); second, covering cartilage with dominant radial fibers (~2/3 of the cartilage thickness in subchondral bone side), R2 (deep layer ROI); and third, covering the entire thickness of the cartilage, R3 (global ROI). Slices were selected by trained MRI image analysts (BN and AMA). Single-component exponential fitting models were used to measure T_2*, T_1, and Adiab$T_{1\rho}$ relaxation times based on published techniques (Y. Ma et al., 2017a; Wu et al., 2019). The acquired UTE-MT data with three saturation pulse power levels and five frequency offsets were used first for MTR calculation and then two-pool MT modeling to calculate MMF and T_2mm (Ma et al., 2018c, 2016; Y. Ma et al., 2017b). In this model, cartilage is assumed to have two different proton pools. The first pool is the macromolecular proton pool (comprised mainly of collagen and PG protons), which has a very broad spectrum and an extremely short T_2 (<20 μs). The second pool is the water proton pool with a much longer T_2. All UTE MRI measurements and models were performed using MATLAB (version 2017, The Mathworks Inc., Natick, MA, USA) codes developed in-house.

2.4. Mechanical indentation testing

Cartilage mechanical properties were measured using a custom-built indentation testing instrument employing a steel indenter with spherical tip (diameter 800 μm) (Chen et al., 2019). Cartilage specimens were washed with PBS after MRI scans and were soaked in PBS for four hours before mechanical tests. Soaking specimens in PBS was assumed to replace potential Fomblin infiltration in the scanned tissues. The bone side of each specimen was fixed in 1-inch petri dishes using a commercial epoxy glue. Indentation tests were performed while specimens were immersed in PBS. Figure 1a shows the indentation test setup measuring the mechanical properties of a representative tibial cartilage specimen. Each specimen was tested at five different points (petri dishes, together with their specimens, were relocated horizontally by the operator), which were selected to be equally distributed within a central circle covering half of the cartilage surface (Figure 1a).

The instrument provided a software-controlled vertical (z-axis) displacement of the indenter with approximately 1-μm positional precision. The device was capable of continuous load measurement with 0.001 N resolution during the indentation test. After finding contact, the actuator lowered the indenter at a rate of 120 μm/sec which is in range of previously reported displacement rates (Tang et al., 2011). The loading was followed by immediate unloading with an unloading rate of 120 μm/sec. Maximum indentation depth was set to be 150 μm (approx. 10% of the cartilage thickness) in order to avoid potential nonlinearities in cartilage deformation and impacts from subchondral bone mechanical properties on the

indentation measures. The average thickness of cartilage samples used in this study ranged from 1.2 to 2.5 mm. The average mechanical properties for each point were measured from two consecutive indentation processes, with five seconds rest time in between. Figure 1b shows the load-displacement curve for a representative indentation test (two consecutive indentations) to measure maximum load (P_{max}), which is required for stiffness (K) and Hayes elastic modulus (E) measurements using Eq.1 and Eq.2 (Hayes et al., 1972). Overlaying the load-displacement curves for the two consecutive indentations illustrated a high repeatability level in mechanical measurement process.

$$K = \frac{P_{max} \cdot Th}{A \cdot w} \quad \text{Eq. 1}$$

$$E = P_{max} \frac{\left(1 - v^2\right)}{2awH}, \quad \text{Eq. 2}$$

where A, ν, a, w, Th, and H are contact area, poison ratio, radius of the indenter, indentation depth, cartilage thickness, and correction factor introduced by Hayes et al. (Hayes et al., 1972), respectively. A Poisson's ratio of 0.45 was used in the calculations, similar to earlier studies focused on human cartilage (Vidal-Lesso et al., 2014).

2.5. Statistical analysis

Average UTE MRI quantifications (T_2*, Adiab$T_{1\rho}$, T_1, and MTR, as well as MMF and T_2mm from two-pool MT modeling) were calculated for each specimen over three middle slices within the superficial layer, deep layer, and global ROIs. Pearson's correlations and linear regression analyses were performed between average UTE MRI quantifications and measured mechanical properties (stiffness and Hayes modulus). All statistical analyses were performed in MATLAB.

3. RESULTS

Figure 2a shows a representative 3D-UTE-Cones MRI (TE=0.032 ms) image of ten tibiofemoral cartilage specimens from the total 40 specimens. Single-component T_2* fitting for one representative cartilage specimen (48-year-old-male) within the global ROI is shown in Figure 2b (T_2*=25.1±2.8 ms). Adiab$T_{1\rho}$ measurement of the same ROI is shown in Figure 2c (Adiab$T_{1\rho}$=51.2±8.2 ms). Figure 2d shows T_1 fitting for the same cartilage specimen, demonstrating a mean T_1 of 779±10 ms. Figure 2e shows the corresponding two-pool MT modeling with fitting lines for 500°, 1000°, and 1500° MT pulse powers depicted in blue, green, and red, respectively. A mean MMF of 9.1±1.0% and a T_2mm of 6.9±0.5 μs were demonstrated.

The average, standard deviation, and the range of the mechanical and UTE MRI quantifications for the studied cartilage specimens within superficial layer, deep layer, and global ROIs are presented in Table 2. A series of MTR values were measured, but only MTR values at 2 kHz frequency offset are presented in the table. Other MTR values showed similar trends.

The average coefficient variation between the mechanical measures of the five locations used in each specimen was 26±12%. However, the average coefficient variation between the two consecutive mechanical measures at each point was <2%.

The Pearson's correlation coefficients between cartilage mechanical properties and UTE MRI measures are presented in Table 3. Correlations of mechanical properties with T_2*, T_1, and T_2mm were non-significant. On average, cartilage mechanical properties demonstrated highest correlations with UTE measures of the superficial layer of cartilage. Adiab$T_{1\rho}$, MTR, and MMF in superficial layer ROIs showed significant correlations with mechanical stiffness ($p<0.05$, $R=-0.51$, 0.47, and 0.64, respectively) and Hayes elastic modulus ($p<0.05$, $R=-0.54$, 0.449, and 0.66, respectively). Adiab$T_{1\rho}$, MTR, and MMF in global ROIs presented significant correlations with mechanical stiffness ($p<0.05$, $R=-0.33$, 0.49, and 0.56, respectively) and Hayes elastic modulus ($p<0.05$, $R=-0.37$, 0.52, and 0.60, respectively).

The scatter plots and linear regression analyses of Adiab$T_{1\rho}$, MTR, and MMF (superficial layer, deep layer, and global ROIs) on cartilage stiffness are illustrated in Figure 3. The scatter plots and linear regression analyses of Adiab$T_{1\rho}$, MTR, and MMF (superficial layer, deep layer, and global ROIs) on Hayes elastic modulus of cartilage specimens are shown in Figure 4.

4. DISCUSSION

This study was the first to investigate correlation of a series of quantitative 3D-UTE-Cones biomarkers (T_2*, Adiab$T_{1\rho}$, T_1, and MTR, as well as MMF and T_2mm from two-pool MT modeling) with human cartilage mechanical properties. UTE-Adiab$T_{1\rho}$ and UTE-MT modeling have demonstrated low sensitivity to the magic angle effect (Ma et al., 2018a, 2016; Wu et al., 2020b, 2020a; Zhu et al., 2018). UTE-MT modeling estimates the amount of cartilage macromolecules (e.g., collagen and PG), a measure which is hypothesized to correlate with cartilage mechanical properties. Prior studies employing conventional $T_{1\rho}$ techniques for cartilage assessment have shown inverse correlation between $T_{1\rho}$ values and PG contents (Jobke et al., 2013; Nishioka et al., 2012); consequently, $T_{1\rho}$ is expected to correlate negatively with cartilage mechanical properties.

Our study of 40 human tibiofemoral cartilage specimens demonstrated significant correlations of UTE-based MMF, MTR, and Adiab$T_{1\rho}$ with mechanical properties (Table 3 and Figure 3 and4) measured with a non-invasive indentation test. The indentation test has been commonly employed to assess mechanical properties of cartilage and meniscus specimens (Antons et al., 2018; Chen et al., 2019; Choi et al., 2016; Jeng et al., 2013; Moshtagh et al., 2016). Since indentation-based mechanical assessment is highly affected by the properties of the tissue located near the surface, higher correlation with mechanical properties was observed for UTE measures in superficial layer ROIs. Among the studied UTE measures, MMF obtained from two-pool UTE-MT modeling demonstrated the highest correlations with cartilage mechanical properties.

A number of studies employing quantitative MR techniques on non-clinical μMRI scanners have been reported for predicting the mechanical properties of cartilage specimens. Nieminen et al. (Nieminen et al., 2004) reported significant correlations between bovine cartilage elastic modulus from compression tests and superficial layer T_2 (20 data points, R=0.62–0.73) as well as delayed gadolinium enhanced T_1 (T_{1Gd}) in global ROIs (32 data points, R=0.70–0.93) performed on a 9.4T μMRI scanner. Wheaton et al. (Wheaton et al., 2005) found significant correlations between bovine cartilage stiffness at equilibrium (i.e., no fluid flow) and average $T_{1\rho}$ of six specimen groups (n=7 per group, R= 0.91) performed on a 4.7 T scanner. Samosky et al. (Samosky et al., 2005) evaluated the relationship between local mechanical properties of three human tibial cartilage samples and their T_{1Gd} values measured on a 8.45T scanner. They reported significant correlation between T_{1Gd} and local mechanical load peaks (indentation tests, 119 data points, R=0.56). Later, Rautiainen et al. (Rautiainen et al., 2015) reported significant correlations between mechanical properties and various quantitative MR properties including T_1, $T_{1\rho}$, $T_{2\rho}$, and MT-saturated T_1 for 14 human tibial cartilage specimens scanned at 9.4T. They also found significant T_1 and $T_{1\rho}$ differences between early and advanced OA specimens.

From studies on clinical MRI scanners, Lammentausta et al. (Lammentausta et al., 2007) reported significant correlations between mechanical properties (via indentation tests) of cadaveric human patellar cartilage specimens and superficial layer T_2 (n=14, R=0.54–0.62) as well as T_2 (R=0.40–0.46) and $T1_{Gd}$ (R=0.30) in global ROIs performed on a 1.5T scanner. Tang et al. (Tang et al., 2011) reported significant correlations between $T_{1\rho}$ values on a 3T scanner and phase angle (7 cadaveric specimens, n=34 data points, R=0.91), a viscoelastic mechanical behavior of cartilage, while correlations with elastic mechanical properties were not significant. Bae et al. (Bae et al., 2014) reported UTE-$T_{1\rho}$ at 3T as a biomarker sensitive to biomechanical softening of human temporomandibular joint discs caused by multiple loading steps. Choi et al. (Choi et al., 2016) found positive correlations between the thickness of lamellar layer visualized in UTE MRI at 3T and the meniscus indentation stiffness (n=9, Spearman's correlation coefficient (SCC)=0.73). Svärd et al. (Svärd et al., 2018) showed that arthroscopic stiffness and T_2 mapping could distinguish between the OA and normal femoral cartilage at 1.5T, however, no significant correlation was observed between T_2 and mechanical properties. Grondin et al. (Grondin et al., 2019) reported significant correlation between cartilage mechanical properties (via compression tests, n=24, R=0.36–0.68) and bound water fraction obtained from multi-component driven equilibrium steady-state observation of T_1 and T_2 (mcDESPOT) measures on a 3T scanner.

Correlation levels of the abovementioned MRI techniques with the mechanical properties of articular cartilage were similar to the correlation levels presented in this study, particularly for studies performed in clinical MRI scanners. However, those MRI techniques based on conventional T_2 or $T_{1\rho}$ measurements are known to be sensitive to the magic angle effect (Li et al., 2011; Shao et al., 2017; Wang and Xia, 2013; Wu et al., 2020b). UTE-Adiab$T_{1\rho}$ and UTE-MT techniques can evaluate both short and long T_2 components in articular cartilage with little sensitivity to the magic angle effect (Ma et al., 2016; Wu et al., 2020b, 2020a; Zhu et al., 2018), and are expected to be more robust in the evaluation of cartilage mechanical properties. Indeed, our preliminary results indicate that MMF from UTE-MT modeling and UTE-Adiab$T_{1\rho}$ are useful and promising surrogates for predicting the mechanical properties

of human articular cartilage. However, UTE biomarkers (MMF, MTR, and UTE-Adiab$T_{1\rho}$) are only moderately correlated with stiffness and Hayes elastic modulus of articular cartilage. The advantages of the presented UTE-MRI measures over conventional biomarkers (T_2, $T_{1\rho}$, T_1, T_{1Gd}, etc.) have yet to be investigated.

The UTE-MT modeling technique has been investigated in previous studies on other MSK tissues and has demonstrated significant correlations with bone microstructural properties (Jerban et al., 2019e, 2019b, 2019d), bone mechanical properties (Jerban et al., 2019a, 2018), and tendon structure (Jerban et al., 2019c; Zhu et al., 2018). The potential of UTE-Adiab$T_{1\rho}$ technique for mechanical and structural assessment of other MSK tissues is yet to be investigated.

The repeatability of the UTE-MT modeling measures was investigated in a prior study performed on lower leg bones of volunteers and resulted in coefficients of variation below 3% (Jerban et al., 2019b). The repeatability of measuring mechanical properties using our in-house indentation test instrument was very high, as the coefficient of variation was below 2% for the two consecutive measurements at each location.

This study has several limitations. First, the number of samples and especially the number of donors were relatively small, limiting the statistical significance. Our samples were from only seven donors, without advanced cartilage degeneration. We were not able to investigate the differences between samples from young and elderly donors for two primary reasons: first, the number of cartilage specimens from young and elderly donors was not similar, and second, specimens were not harvested from the same location in the tibiofemoral cartilage. Consequently, investigating the intra-donor and inter-donor differences in MRI and mechanical properties was not possible. The inclusion of more samples with more advanced degeneration is expected to increase the statistical significance of this study. Since all specimens selected in this study were macroscopically normal, soaking specimens in PBS for four hours after MR imaging did not result in any considerable swelling, A shorter PBS soaking time should be an important consideration when specimens are more degenerated (as will be the case in future studies). Second, MMF has been compared with single-component relaxation times (T_{2*}, T_1, $T_{1\rho}$). Bi-component fitting analyses were not performed in this study due to the limited acquired data points. Well-designed future studies should be focused on investigating other UTE-MRI parameters with potential low sensitivity to magic angle effect. Such UTE-MRI parameters (for instance, the fraction of short $T_{2*}/T_{1\rho}$ component) can be developed using bi-component fitting analyses (Qian et al., 2010; Shao et al., 2016; Sharafi et al., 2017). Third, histological analysis was not performed, so the degree of degeneration for each cartilage sample was unknown. Fourth, this study was performed ex vivo on tibiofemoral cartilage specimens where surrounding muscle and synovium liquid were not present. An in vivo study should be performed to examine correlations between UTE-MT measurements and cartilage mechanical properties (via arthroscopic indentation). In vivo MMF correlations with mechanical properties could also be affected by subject motion during the MRI scan (Wu et al., 2019) and by difference in temperature between the body and standard room conditions (Jerban et al., 2019f). The fifth limitation of this study was the long scan time. Employing different accelerating techniques, such as stretching the cones readout trajectory (Wan et al., 2019) or advanced image reconstruction techniques,

such as parallel imaging and compressed sensing (Otazo et al., 2010), may help reducing the total scan time.

5. Conclusions

A series of 3D-UTE-Cones biomarkers, including T_2*, T_1, Adiab$T_{1\rho}$, MTR, MMF, and T_2mm were investigated for their capacities to predict mechanical properties of human tibiofemoral cartilage in an ex vivo study. MMF, MTR, and Adiab$T_{1\rho}$ measured in the superficial layer and global ROI of cartilage demonstrated significant correlations with stiffness and Hayes elastic modulus, as measured with an indentation test. On average, mechanical properties showed higher correlations with UTE measures in the superficial layer ROI. Of the studied biomarkers, MMF showed the highest correlations with cartilage mechanical properties. This study highlighted the UTE-MT technique for assessment of mechanical properties of tibiofemoral cartilage.

Acknowledgement

The authors acknowledge grant support from NIH (R01AR075825, 2R01AR062581, 1R01AR068987, 1R21 AR075851), VA Clinical Science and Rehabilitation R&D Awards (I01CX001388 and I01RX002604), and Shaffer Family Foundation.

Abbreviations:

MR	magnetic resonance
MRI	magnetic resonance imaging
3D	three-dimensional
UTE	three-dimensional ultrashort echo time imaging
RF	radio frequency
FOV	field of view
ROI	region of interest
TE	echo time
TR	repetition time
MT	magnetization transfer
MTR	magnetization transfer ratio
MMF	macromolecular fraction
T2mm	macromolecular T2
FA	flip angle
TSL	Spin-locking time

AFP	adiabatic full passage
AFI-VTR	actual flip angle imaging with variable
PBS	phosphate buffered saline

8. References

Antons J, Marascio MGM, Nohava J, Martin R, Applegate LA, Bourban PE, Pioletti DP, 2018 Zone-dependent mechanical properties of human articular cartilage obtained by indentation measurements. J. Mater. Sci. Mater. Med 29 10.1007/s10856-018-6066-0

Bae WC, Biswas R, Chen K, Chang EY, Chung CB, Bae C, 2014 UTE MRI of the Osteochondral Junction Compliance with Ethics Guidelines Conflict of Interest Won. Curr Radiol Rep Febr 1, 1–20. 10.1007/s40134-013-0035-7

Bredella MA, Tirman PF, Peterfy CG, Zarlingo M, Feller JF, Bost FW, Belzer JP, Wischer TK, Genant HK, 1999 Accuracy of T2-weighted fast spin-echo MR imaging with fat saturation in detecting cartilage defects in the knee: comparison with arthroscopy in 130 patients. Am. J. Roentgenol 172, 1073–1080. 10.2214/ajr.172.4.10587150 [PubMed: 10587150]

Carl M, Bydder GM, Du J, 2016 UTE imaging with simultaneous water and fat signal suppression using a time-efficient multispoke inversion recovery pulse sequence. Magn. Reson. Med 76, 577–582. 10.1002/mrm.25823 [PubMed: 26309221]

Chang EY, Du J, Chung CB, 2015 UTE imaging in the musculoskeletal system. J. Magn. Reson. Imaging 41, 870–883. 10.1002/jmri.24713 [PubMed: 25045018]

Chang EY, Ma Y, Du J, 2016 MR Parametric Mapping as a Biomarker of Early Joint Degeneration. Sport. Heal. A Multidiscip. Approach 8, 405–411. 10.1177/1941738116661975

Chen B, Cheng X, Dorthe EW, Zhao Y, D'Lima D, Bydder GM, Liu S, Du J, Ma YJ, 2019 Evaluation of normal cadaveric Achilles tendon and enthesis with ultrashort echo time (UTE) magnetic resonance imaging and indentation testing. NMR Biomed 32, e4034 10.1002/nbm.4034 [PubMed: 30457179]

Choi J-YY, Biswas R, Bae WC, Healey R, Im M, Statum S, Chang EY, Du J, Bydder GM, D'lima D, Chung CB, D'Lima D, Chung CB, 2016 Thickness of the meniscal lamellar layer: Correlation with indentation stiffness and comparison of normal and abnormally thick layers by using multiparametric ultrashort echo time MR imaging. Radiology 280, 161–168. 10.1148/radiol.2016150633 [PubMed: 26829523]

Du J, Takahashi AM, Chung CB, 2009 Ultrashort TE spectroscopic imaging (UTESI): Application to the imaging of short T2 relaxation tissues in the musculoskeletal system. J. Magn. Reson. Imaging 29, 412–421. 10.1002/jmri.21465 [PubMed: 19161197]

Grondin M, Liu F, Vignos M, Du J, Henak C, Kijowski R, 2019 Comparison of Single-Component and Multi- Component T2 Parameters and Mechanical Parameters of Human Patellar Cartilage at 3. 0T, in: The International Society for Magnetic Resonance in Medicine (ISMRM) p. Poster 1329.

Guermazi A, Roemer FW, Burstein D, Hayashi D, 2011 Why radiography should no longer be considered a surrogate outcome measure for longitudinal assessment of cartilage in knee osteoarthritis. Arthritis Res. Ther 13, 247 10.1186/ar3488 [PubMed: 22136179]

Gurney PT, Hargreaves BA, Nishimura DG, 2006 Design and analysis of a practical 3D cones trajectory. Magn. Reson. Med 55, 575–582. 10.1002/mrm.20796 [PubMed: 16450366]

Hayes WC, Keer LM, Herrmann G, Mockros LF, 1972 A mathematical analysis tests of articular cartilage. J. Biomech 5, 541–551. [PubMed: 4667277]

Heinegård D, Saxne T, 2011 The role of the cartilage matrix in osteoarthritis. Nat. Rev. Rheumatol 7, 50–56. 10.1038/nrrheum.2010.198 [PubMed: 21119607]

Helmick CG, Felson DT, Lawrence RC, Gabriel S, Hirsch R, Kwoh CK, Liang MH, Kremers HM, Mayes MD, Merkel PA, Pillemer SR, Reveille JD, Stone JH, 2008 Estimates of the prevalence of arthritis and other rheumatic conditions in the United States. Part I. Arthritis Rheum 58, 15–25. 10.1002/art.23177 [PubMed: 18163481]

Jeng YR, Mao CP, Wu K. Te, 2013 Instrumented indentation investigation on the viscoelastic properties of porcine cartilage. J. Bionic Eng 10.1016/S1672-6529(13)60239-5

Jerban S, Ma Y, Dorthe EW, Kakos L, Le N, Alenezi S, Sah RL, Chang EY, D'Lima D, Du J, 2019a Assessing cortical bone mechanical properties using collagen proton fraction from ultrashort echo time magnetization transfer (UTE-MT) MRI modeling. Bone Reports 8 10.1016/j.bonr.2019.100220

Jerban S, Ma Y, Li L, Jang H, Wan L, Guo T, Searleman A, Chang EY, Du J, 2019b Volumetric Mapping of Bound and Pore Water as well as Collagen Protons in Cortical Bone Using 3D Ultrashort Echo Time Cones MR Imaging Techniques. Bone 127, 120–128. 10.1016/j.bone.2019.05.038 [PubMed: 31176044]

Jerban S, Ma Y, Namiranian B, Ashir A, Shirazian H, Zhao W, Wu M, Cai Z, Le N, Du J, Chang EY, 2019c Age-related decrease in collagen proton fraction in tibial tendons estimated by magnetization transfer modeling of ultrashort echo time magnetic resonance imaging (UTE-MRI). Sci. Rep 11, 1–8. [PubMed: 30626917]

Jerban S, Ma Y, Nazaran A, Dorthe EW, Cory E, Carl M, D'Lima D, Sah RL, Chang EY, Du J, D'Lima D, Sah RL, Chang EY, Du J, 2018 Detecting stress injury (fatigue fracture) in fibular cortical bone using quantitative ultrashort echo time-magnetization transfer (UTE-MT): An ex vivo study. NMR Biomed 31, e3994 10.1002/nbm.3994 [PubMed: 30059184]

Jerban S, Ma Y, Wan L, Searleman AC, Jang H, Sah RL, Chang EY, Du J, 2019d Collagen proton fraction from ultrashort echo time magnetization transfer (UTE-MT) MRI modelling correlates significantly with cortical bone porosity measured with micro-computed tomography (μCT). NMR Biomed 32, e4045 10.1002/nbm.4045 [PubMed: 30549338]

Jerban S, Ma Y, Wong JH, Nazaran A, Searleman A, Wan L, Williams J, Du J, Chang EY, 2019e Ultrashort echo time magnetic resonance imaging (UTE-MRI) of cortical bone correlates well with histomorphometric assessment of bone microstructure. Bone 123, 8–17. 10.1016/j.bone.2019.03.013 [PubMed: 30877070]

Jerban S, Szeverenyi N, Ma Y, Guo T, Namiranian B, To S, Jang H, Eric Y Chang Du, J., 2019f Ultrashort echo time MRI (UTE-MRI) quantifications of cortical bone varied significantly at body temperature compared with room temperature. Investig. Magn. Reson. Imaging 23, 00 10.13104/imri.2019.23.3.000

Jobke B, Bolbos R, Saadat E, Cheng J, Li X, Majumdar S, 2013 Mechanism of disease in early osteoarthritis: Application of modern MR imaging techniques - a technical report. Magn. Reson. Imaging 31, 156–161. 10.1016/j.mri.2012.07.005 [PubMed: 22902064]

Juras V, Zbyn S, Pressl C, Valkovic L, Szomolanyi P, Frollo I, Trattnig S, 2012 Regional variations of T2* in healthy and pathologic achilles tendon in vivo at 7 Tesla: Preliminary results. Magn. Reson. Med. 68, 1607–1613. 10.1002/mrm.24136 [PubMed: 22851221]

Kleeman RU, Krocker D, Cedrano A, Tuischer J, Duda GN, 2005 Altered cartilage mechanics and histology in knee osteoarthritis: Relation to clinical assessment (ICRS Grade). Osteoarthr. Cartil 13, 958–963. 10.1016/j.joca.2005.06.008

Laasanen MS, Töyräs J, Korhonen RK, Rieppo J, Saarakkala S, Nieminen MT, Hirvonen J, Jurvelin JS, 2003 Biomechanical properties of knee articular cartilage. Biorheology 40, 133–40. [PubMed: 12454397]

Lammentausta E, Kiviranta P, Töyräs J, Hyttinen MM, Kiviranta I, Nieminen MT, Jurvelin JS, 2007 Quantitative MRI of parallel changes of articular cartilage and underlying trabecular bone in degeneration. Osteoarthr. Cartil 15, 1149–1157. 10.1016/j.joca.2007.03.019

Li W, Hong L, Hu L, Magin RL, 2010 Magnetization Transfer Imaging Provides a Quantitative Measure of Chondrogenic Differentiation and Tissue Development. Tissue Eng. Part C Methods 16, 1407–1415. 10.1089/ten.tec.2009.0777 [PubMed: 20373975]

Li X, Cheng J, Lin K, Saadat E, Bolbos RI, Jobke B, Ries MD, Horvai A, Link TM, Majumdar S, 2011 Quantitative MRI using T1ρ and T2 in human osteoarthritic cartilage specimens: Correlation with biochemical measurements and histology. Magn. Reson. Imaging 29, 324–334. 10.1016/j.mri.2010.09.004 [PubMed: 21130590]

Ma Y, Carl M, Searleman A, Lu X, Chang EY, Du J, 2018a 3D adiabatic T1ρprepared ultrashort echo time cones sequence for whole knee imaging. Magn. Reson. Med 80, 1429–1439. 10.1002/mrm.27131 [PubMed: 29493004]

Ma Y, Carl M, Shao H, Tadros AS, Chang EY, Du J, 2017a Three-dimensional ultrashort echo time cones T 1ρ (3D UTE-cones-T 1ρ) imaging. NMR Biomed 30, e3709 10.1002/nbm.3709

Ma Y, Chang EY, Carl M, Du J, 2017b Quantitative magnetization transfer ultrashort echo time imaging using a time-efficient 3D multispoke Cones sequence. Magn. Reson. Med 79, 692–700. 10.1002/mrm.26716 [PubMed: 28470838]

Ma Y, Lu X, Carl M, Zhu Y, Szeverenyi NM, Bydder GM, Chang EY, Du J, 2018b Accurate T 1 mapping of short T 2 tissues using a three-dimensional ultrashort echo time cones actual flip angle imaging-variable repetition time (3D UTE-Cones AFI-VTR) method. Magn. Reson. Med 80, 598–608. 10.1002/mrm.27066 [PubMed: 29314235]

Ma Y, Shao H, Du J, Chang EY, 2016 Ultrashort echo time magnetization transfer (UTE-MT) imaging and modeling: magic angle independent biomarkers of tissue properties. NMR Biomed 29, 1546–1552. 10.1002/nbm.3609 [PubMed: 27599046]

Ma Y, Tadros A, Du J, Chang EY, 2018c Quantitative two-dimensional ultrashort echo time magnetization transfer (2D UTE-MT) imaging of cortical bone. Magn. Reson. Med 79, 1941–1949. 10.1002/mrm.26846 [PubMed: 28776754]

Ma YJ, Zhu Y, Lu X, Carl M, Chang EY, Du J, 2017 Short T 2 imaging using a 3D double adiabatic inversion recovery prepared ultrashort echo time cones (3D DIR-UTE-Cones) sequence. Magn. Reson. Med 00, 1–9. 10.1002/mrm.26908

Mosher TJ, Zhang Z, Reddy R, Boudhar S, Milestone BN, Morrison WB, Kwoh CK, Eckstein F, Witschey WRT, Borthakur A, 2011 Knee Articular Cartilage Damage in Osteoarthritis: Analysis of MR Image Biomarker Reproducibility in ACRIN-PA 4001 Multicenter Trial. Radiology 258, 832–842. 10.1148/radiol.10101174 [PubMed: 21212364]

Moshtagh PR, Pouran B, Korthagen NM, Zadpoor AA, Weinans H, 2016 Guidelines for an optimized indentation protocol for measurement of cartilage stiffness: The effects of spatial variation and indentation parameters. J. Biomech 49, 3602–3607. 10.1016/j.jbiomech.2016.09.020 [PubMed: 27660171]

Nieminen MT, Töyräs J, Laasanen MS, Silvennoinen J, Helminen HJ, Jurvelin JS, 2004 Prediction of biomechanical properties of articular cartilage with quantitative magnetic resonance imaging. J. Biomech 37, 321–328. 10.1016/S0021-9290(03)00291-4 [PubMed: 14757451]

Nishioka H, Hirose J, Nakamura E, Oniki Y, Takada K, Yamashita Y, Mizuta H, 2012 T 1ρ and T 2 mapping reveal the in vivo extracellular matrix of articular cartilage. J. Magn. Reson. Imaging 35, 147–155. 10.1002/jmri.22811 [PubMed: 21990043]

Otazo R, Kim D, Axel L, Sodickson DK, 2010 Combination of compressed sensing and parallel imaging for highly accelerated first-pass cardiac perfusion MRI. Magn. Reson. Med 64, 767–776. 10.1002/mrm.22463 [PubMed: 20535813]

Palmoski MJ, Brandt KD, 1981 Running Inhibits the Reversal of Atrophic Changes in Canine Knee Cartilage After Removal of a Leg Cast. Arthritis Rheum 24, 1329–1337. 10.1002/art.1780241101 [PubMed: 7317111]

Qian Y, Williams AA, Chu CR, Boada FE, 2010 Multicomponent T2* mapping of knee cartilage: Technical feasibility ex vivo. Magn. Reson. Med 64, 1427–1432. 10.1002/mrm.22450

Rautiainen J, Nissi MJ, Salo E-N, Tiitu V, Finnilä M. a J., Aho O-M, Saarakkala S, Lehenkari P, Ellermann J, Nieminen MT, 2015 Multiparametric MRI assessment of human articular cartilage degeneration: Correlation with quantitative histology and mechanical properties. Magn. Reson. Med 74, 249–259. 10.1002/mrm.25401 [PubMed: 25104181]

Recht MP, Goodwin DW, Winalski CS, White LM, 2005 MRI of Articular Cartilage: Revisiting Current Status and Future Directions. Am. J. Roentgenol 185, 899–914. 10.2214/ajr.05.0099 [PubMed: 16177408]

Samosky JT, Burstein D, Grimson WE, Howe R, Martin S, Gray ML, 2005 Spatially-localized correlation of dGEMRIC-measured GAG distribution and mechanical stiffness in the human tibial plateau. J. Orthop. Res 23, 93–101. 10.1016/j.orthres.2004.05.008 [PubMed: 15607880]

Shao H, Chang EY, Pauli C, Zanganeh S, Bae WC, Chung CB, Tang G, Du J, 2016 UTE bi-component analysis of T2* relaxation in articular cartilage. Osteoarthr. Cartil 24, 364–373. 10.1016/j.joca.2015.08.017

Shao H, Pauli C, Li S, Ma Y, Tadros AS, Kavanaugh A, Chang EY, Tang G, Du J, 2017 Magic angle effect plays a major role in both T1rho and T2 relaxation in articular cartilage. Osteoarthr. Cartil 25, 2022–2030. 10.1016/j.joca.2017.01.013

Sharafi A, Chang G, Regatte RR, 2017 Bi-component T1ρ and T2 Relaxation Mapping of Skeletal Muscle In-Vivo. Sci. Rep 7 10.1038/s41598-017-14581-9

Sophia Fox a. J., Bedi a., Rodeo S. a., 2009 The Basic Science of Articular Cartilage: Structure, Composition, and Function. Sport. Heal. A Multidiscip. Approach 1, 461–468. 10.1177/1941738109350438

Svärd T, Lakovaara M, Pakarinen H, Haapea M, Kiviranta I, Lammentausta E, Jurvelin J, Tervonen O, Ojala R, Nieminen M, 2018 Quantitative MRI of Human Cartilage In Vivo: Relationships with Arthroscopic Indentation Stiffness and Defect Severity. Cartilage 9, 46–54. 10.1177/1947603516684592 [PubMed: 29219019]

Tang SY, Souza RB, Ries M, Hansma PK, Alliston T, Li X, 2011 Local Tissue Properties of Human Osteoarthritic Cartilage Correlate with Magnetic Resonance T 1 rho Relaxation Times. J. Orthop. Res 29, 1312–1319. 10.1002/jor.21381 [PubMed: 21445940]

Vidal-Lesso A, Ledesma-Orozco E, Daza-Benítez L, Lesso-Arroyo R, 2014 Mechanical Characterization of Femoral Cartilage Under Unicompartimental Osteoarthritis. Ing. mecánica, Tecnol. y Desarro 4, 239–246.

Wan L, Zhao W, Ma Y, Jerban S, Searleman AC, Carl M, Chang EY, Tang G, Du J, 2019 Fast quantitative 3D ultrashort echo time MRI of cortical bone using extended cones sampling. Magn. Reson. Med 82, 225–236. 10.1002/mrm.27715 [PubMed: 30821032]

Wang N, Xia Y, 2013 Experimental Issues in the Measurement of Multi-component Relaxation Times in Articular Cartilage by Microscopic MRI Nian. J. Magn. Reson 235, 15–25. 10.1016/j.jmr.2013.07.001.Experimental [PubMed: 23916991]

Wheaton AJ, Dodge GR, Elliott DM, Nicoll SB, Reddy R, 2005 Quantification of cartilage biomechanical and biochemical properties viaT1ρ magnetic resonance imaging. Magn. Reson. Med 54, 1087–1093. 10.1002/mrm.20678 [PubMed: 16200568]

Wu M, Kasibhatala A, Ma Y. jun, Jerban S, Chang Eric Y., Du J, 2020a Magic angle effect on adiabatic T1ρ imaging of the Achilles tendon using 3D ultrashort echo time cones trajectory. NMR Biomed 30, 1–10.

Wu M, Ma Y, Kasibhatla A, Chen M, Jang H, Jerban S, Chang EY, Du J, 2020b Convincing evidence for magic angle less-sensitive quantitative T 1ρ imaging of articular cartilage using the 3D ultrashort echo time cones adiabatic T 1ρ (3D UTE cones-AdiabT 1ρ) sequence. Magn. Reson. Med 1, 1–8. 10.1002/mrm.28317

Wu M, Zhao W, Wan L, Kakos L, Li L, Jerban S, Jang H, Chang EY, Du J, Ma YJ, 2019 Quantitative three-dimensional ultrashort echo time cones imaging of the knee joint with motion correction. NMR Biomed 1–11. 10.1002/nbm.4214

Yelin E, Callahan LF, 1995 the economic cost and social and psychological impact of musculoskeletal conditions. Arthritis Rheum 38, 1351–1362. 10.1002/art.1780381002 [PubMed: 7575685]

Zhu Y, Cheng X, Ma Y, Wong JH, Xie Y, Du J, Chang EY, 2018 Rotator cuff tendon assessment using magic-angle insensitive 3D ultrashort echo time cones magnetization transfer (UTE-Cones-MT) imaging and modeling with histological correlation. J. Magn. Reson. Imaging 48, 160–168. 10.1002/jmri.25914 [PubMed: 29219218]

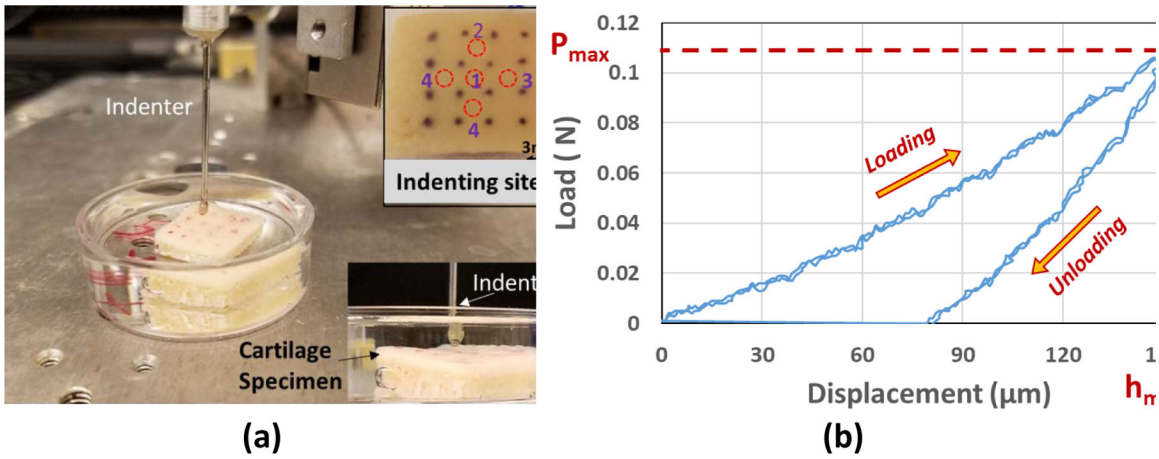

Figure 1.

(a) Experimental setup for indentation test performed on a representative human tibial cartilage. The indenter was machined out of steel, and its tip was spherical (diameter 0.8mm). Five locations were indented on the cartilage surface, and average results were used for each specimen. (b) Load-displacement curve indicating the loading and unloading processes at a displacement rate of120µm/s (maximum indentation depth was 150 µm, assuming one tenth of the average cartilage thickness). Overlaying load-displacement curves for two indentation processes showed the high repeatability level of the mechanical measurement (average coefficient of variation <2%).

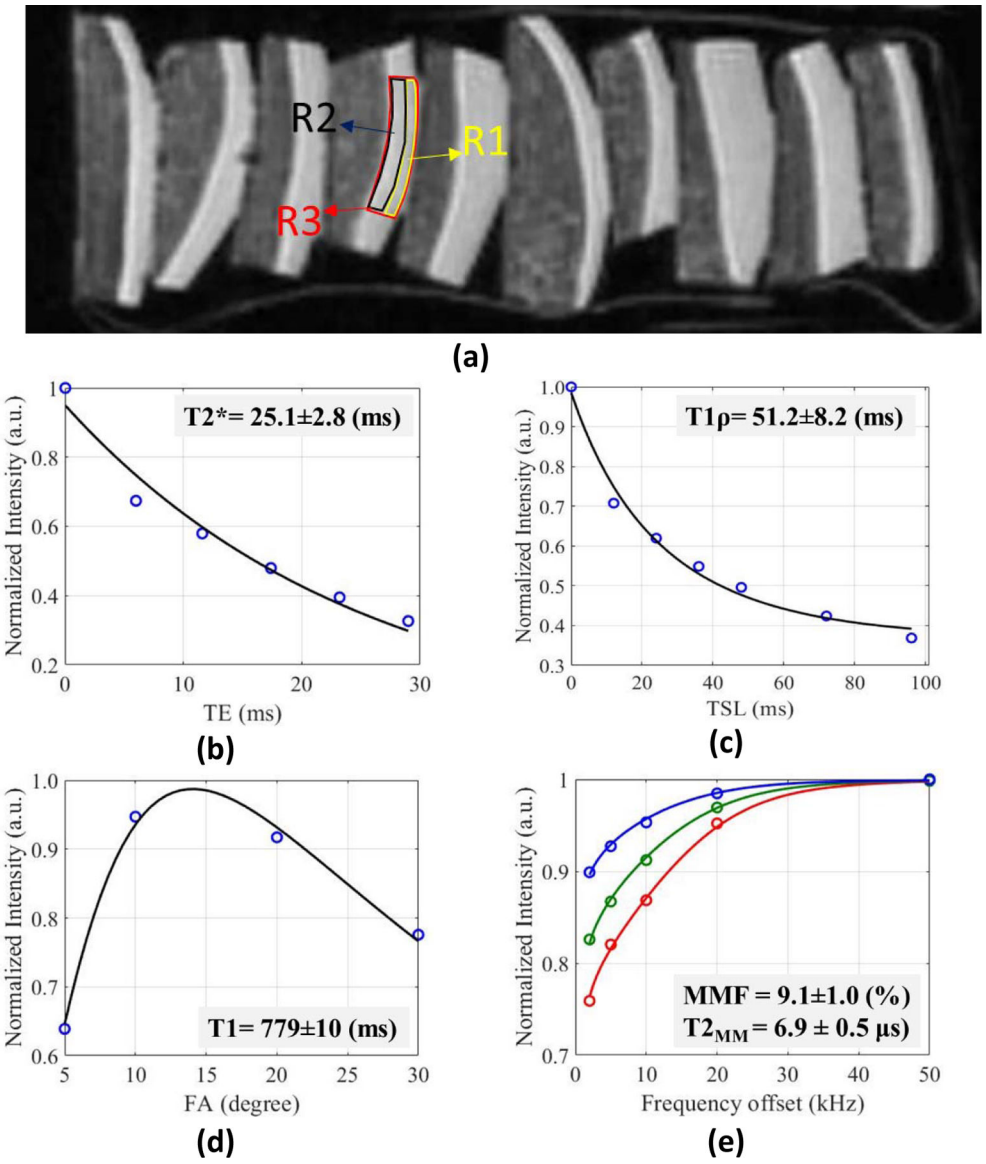

Figure 2.

(a) UTE MRI (TE=0.032 ms, TR=500ms, and FA=10°) image of ten tibiofemoral cartilage specimens scanned in a plastic container filled with fomblin (with no MRI signal). R1, R2, and R3 are representative regions of interest (ROIs) covering the superficial layer, deep layer, and total thickness of the cartilage, respectively. (b) T_2* single-component exponential fitting (signal decay vs. differing TEs) for a representative cartilage specimen (48-year-old-male indicated in Fig 2a) within R3, covering the entire cartilage thickness (global ROI). (c) Adiab$T_{1\rho}$ single-component exponential fitting (Adiab$T_{1\rho}$ signal decay vs. differing spin-lock time, TSL) for the same ROI. (d) T_1 single-component exponential fitting for the same ROI. (e) The two-pool MT modeling analysis using three pulse saturation power levels (500° in blue, 1000° in green, and 1500° in red) and five frequency offsets (2, 5, 10, 20, 50 kHz). MMF and T_2mm refer to macromolecular fraction and macromolecular T_2, respectively.

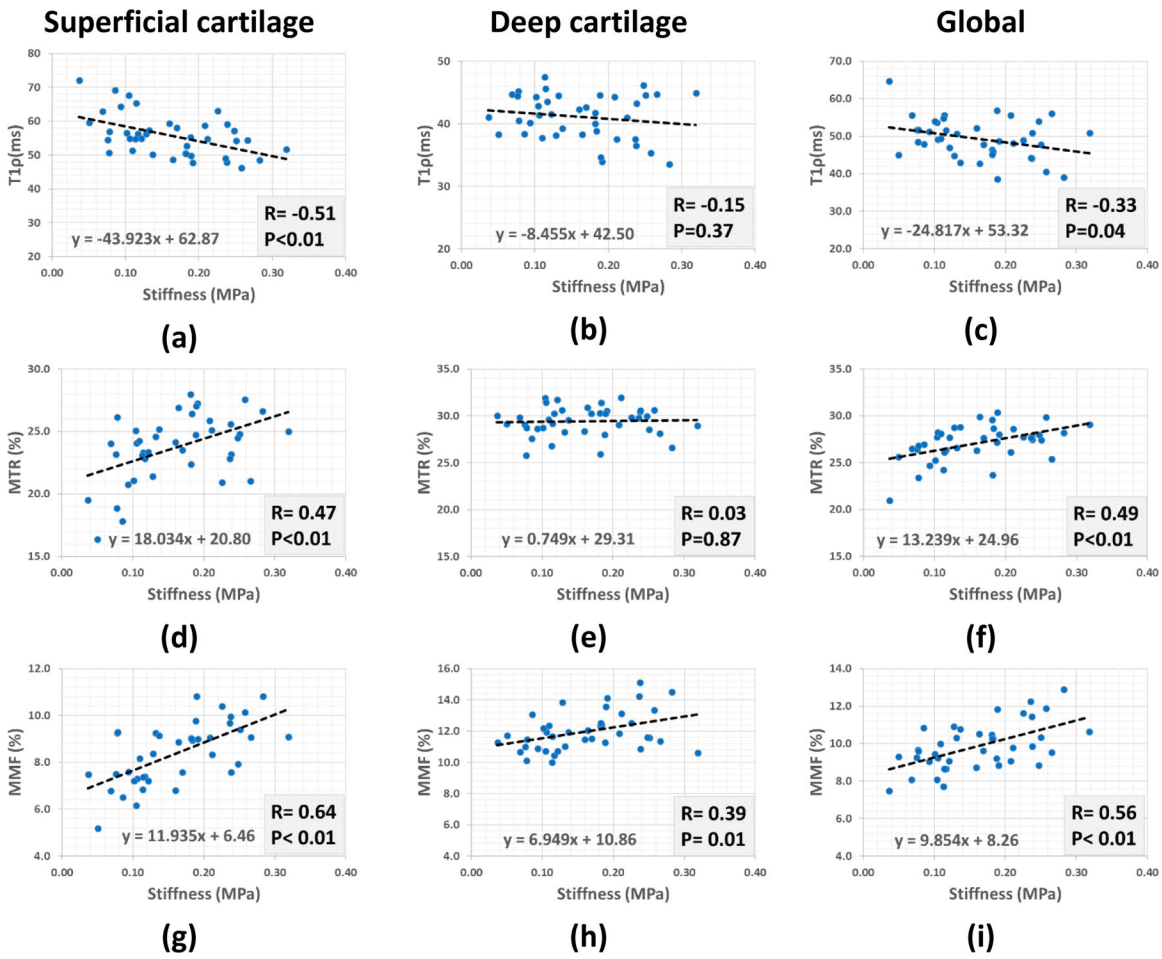

Figure 3.

Scatter plots and linear regression analyses of (a, b, c) Adiab$T_{1\rho}$, (d, e, f) MTR (1000° power and 2KHz frequency offset), and (g, h, i) MMF on cartilage stiffness. MRI measures were performed in (a, d, g) superficial layer, (b, e, h) deep layer, and (c, f, i) global ROIs.

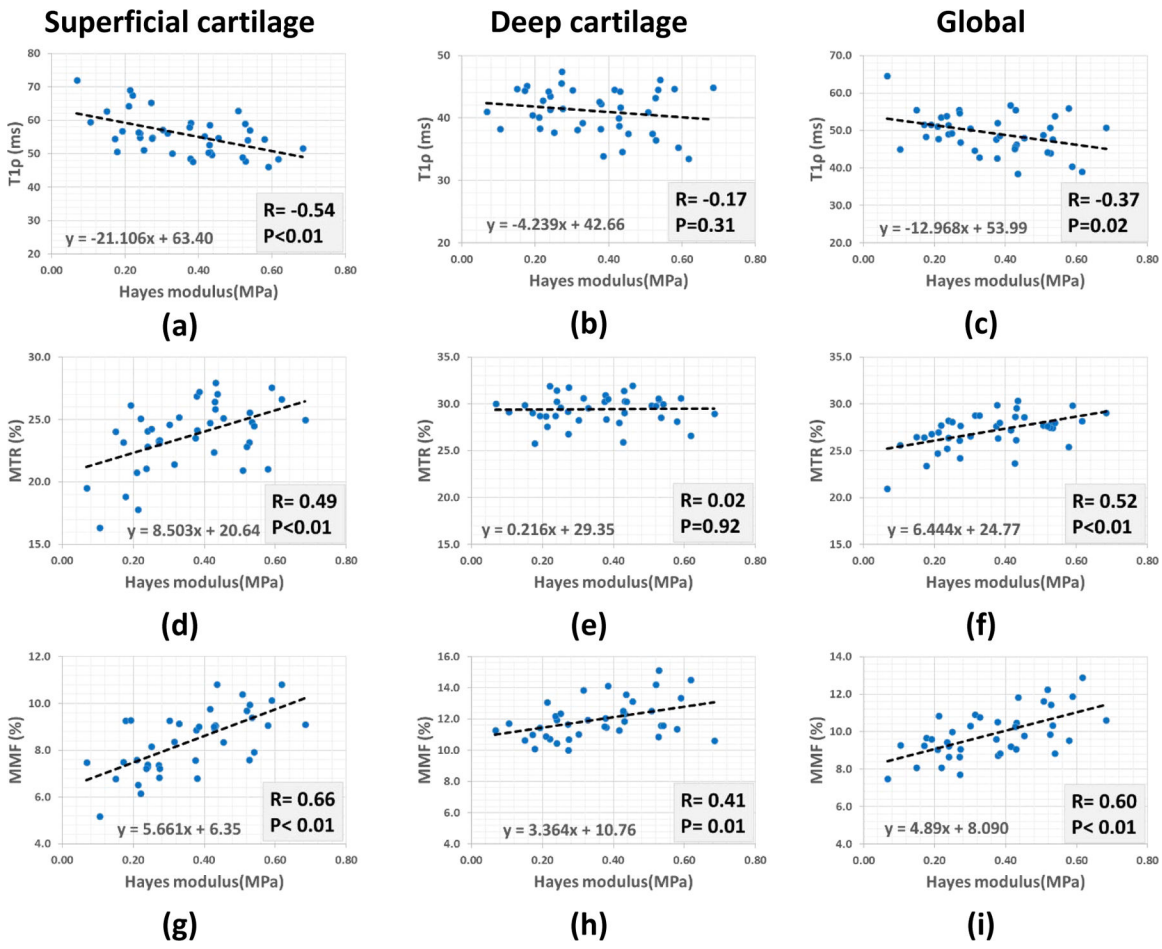

Figure 4.

Scatter plots and linear regression analyses of (a, b, c) Adiab$T_{1\rho}$, (d, e, f) MTR (1000° power and 2KHz frequency offset), and (g, h, i) MMF on Hayes elastic modulus of cartilage. MRI measures were performed in (a, d, g) superficial layer, (b, e, h) deep layer, and (c, f, i) global ROIs.

Table 1:

Summarized MRI sequence parameters

Sequence	TRs/TEs/TSL (ms); FA (°); Saturation pulse power, Θ (°); frequency offset, Δf (KHz)	Other parameters	Scan time (min)
3D-UTE-Cones T_2*	TR=100; TEs= 0.032, 6.0, 11.6, 17.4, 3.2, 29.0; FA =10		6
3D-UTE-Cones Adiab$T_{1\rho}$	TR = 500; TSL = 0, 12, 24, 36, 48, 72 and 96; FA =10	FOV = 110 mm2 Matrix = 300×300 Slice thickness = 0.8 mm Number of slices = 36 Receiver bandwidth = ±62.5 kHz	30
AFI-VTR 3D-UTE-Cones T1	AFI: TE = 0.032; TRs = 20 and 100; FA = 45; VFA: TE = 0.032; TRs = 20; FA = 5, 10, 20, 30;		30
3D-UTE-Cones MT	TR=103, Θ = 500, 1000, and 1500; Δf = 2, 5, 10, 20, and 50; FA = 7;		25

Table 2:

Average, standard deviation, and range of the mechanical and UTE MRI properties in the studied cartilage specimens.

	T_2^* (ms)	T_1 (ms)	Adiab$T_{1\rho}$ (ms)	MTR −15–2* (%)	MTR −10–2* (%)	MTR −5–2* (%)	MMF (%)	T_2mm (μs)	Hayes modulus (MPa)	Stiffness (MPa)
Superficial layer	32.1±8.5 [21,59]	791±115 [640,1103]	55.8±6.1 [46.3,72.1]	29±3 [21,35]	24±3 [16,28]	11±1 [6,13]	8.4±1.3 [5.2,10.8]	6.9±0.4 [6.2,8.0]		
Deep layer	28.8±7.7 [14.7,50.3]	686±69 [491,801]	41.1±3.6 [33.5,47.5]	36±2 [31,39]	29±2 [26,32]	14±1 [11,16]	12.0±1.2 [10,15]	6.9±0.2 [6.4,7.4]	0.39±0.17 [0.07,0.88]	0.17±0.10 [0.04,0.54]
Global	30.1±9.2 [19,59]	773±79 [565,919]	49.3±5.3 [38.6,64.7]	33±2 [26,37]	27±2 [21,30]	13±1 [10,15]	9.9±1.3 [7.5,13.1]	6.9±0.3 [6.3,7.7]		

*MTR-15–2, MTR-10–2, and MTR-5–2 refer to magnetization ratios at 2 kHz frequency offset for 1500, 1000, and 500° pulse power levels, respectively.

Table 3:

Pearson's correlation coefficients between mechanical properties and UTE MRI.

		T_2*	T_1	Adiab$T_{1\rho}$	MTR −15–2*	MTR −10–2*	MTR −5–2*	MMF	T_2mm
Superficial layer	Hayes modulus	0.07 P=0.68	−0.20 P=0.21	−0.54 P<0.01	0.40 P<0.01	0.49 P<0.01	0.35 P=0.03	0.66 P<0.01	−0.25 P=0.12
	Stiffness	0.05 P=0.76	−0.20 P=0.21	−0.51 P<0.01	0.38 P=0.01	0.47 P<0.01	0.34 P=0.03	0.64 P<0.01	−0.22 P=0.25
Deep layer	Hayes modulus	0.09 P=0.59	−0.31 P=0.05	−0.17 P=0.31	0.01 P=0.93	0.02 P=0.92	0.02 P=0.88	0.41 P=0.01	−0.29 P=0.07
	Stiffness	0.12 P=0.47	−0.27 P=0.09	−0.15 P=0.37	0.01 P=0.98	0.03 P=0.87	0.04 P=0.83	0.39 P=0.01	−0.27 P=0.09
Global	Hayes modulus	0.03 P=0.84	−0.26 P=0.11	−0.37 P=0.02	0.44 P<0.01	0.52 P<0.01	0.25 P=0.12	0.60 P<0.01	−0.21 P=0.19
	Stiffness	0.03 P=0.86	−0.22 P=0.17	−0.33 P=0.04	0.42 P<0.01	0.49 P<0.01	0.22 P=0.17	0.56 P<0.01	−0.19 P=0.25

* MTR-15–2, MTR-10–2, and MTR-5–2 refer to magnetization ratios at 2 kHz frequency offset for 1500, 1000, and 500° pulse power levels, respectively.